

Available online at www.sciencedirect.com

ScienceDirect

journal homepage: www.elsevier.com/locate/burns

Uncultured adipose-derived regenerative cells (ADRCs) seeded in collagen scaffold improves dermal regeneration, enhancing early vascularization and structural organization following thermal burns

Philippe Foubert^{a,*}, Samuel Barillas^a, Andreina D. Gonzalez^a, Zeni Alfonso^a, Sherry Zhao^a, Isaac Hakim^b, Carol Meschter^b, Mayer Tenenhaus^c, John K. Fraser^a

^a Cytori Therapeutics Inc, San Diego, CA, USA

^b Comparative Biosciences Inc., Sunnyvale, CA, USA

^c UCSD Medical Center, University of California, San Diego, CA, USA

ARTICLE INFO

Article history:

Received 19 November 2014

Received in revised form

5 May 2015

Accepted 8 May 2015

Available online xxx

Keywords:

Adipose-derived regenerative cells

Thermal burn

Integra[®]

Angiogenesis

ABSTRACT

Objective: Advances in tissue engineering have yielded a range of both natural and synthetic skin substitutes for burn wound healing application. Long-term viability of tissue-engineered skin substitutes requires the formation and maturation of neo-vessels to optimize survival and biointegration after implantation. A number of studies have demonstrated the capacity of Adipose Derived Regenerative Cells (ADRCs) to promote angiogenesis and modulate inflammation. On this basis, it was hypothesized that adding ADRCs to a collagen-based matrix (CBM) (i.e. Integra[®]) would enhance formation and maturation of well-organized wound tissue in the setting of acute thermal burns. The purpose of this study was to evaluate whether seeding uncultured ADRCs onto CBM would improve matrix properties and enhance healing of the grafted wound.

Methods: Full thickness thermal burns were created on the backs of 8 Gottingen mini-swine. Two days post-injury wounds underwent fascial excision and animals were randomized to receive either Integra[®] seeded with either uncultured ADRCs or control vehicle. Wound healing assessment was performed by digital wound imaging, histopathological and immunohistochemical analyses.

Results: In vitro analysis demonstrated that freshly isolated ADRCs adhered and propagated on the CBM. Histological scoring revealed accelerated maturation of wound bed tissue in wounds receiving ADRCs-loaded CBM compared to vehicle-loaded CBM. This was associated with a significant increase in depth of the wound bed tissue and collagen deposition ($p < 0.05$). Blood vessel density in the wound bed was 50% to 69.6% greater in wounds receiving ADRCs-loaded CBM compared to vehicle-loaded CBM ($p = 0.05$) at day 14 and 21. In

* Corresponding author. Tel.: +1 858 458 0900.

E-mail address: pfoubert@cytori.com (P. Foubert).

Abbreviations: ADRCs, adipose-derived regenerative cells; CBM, collagen-based matrix; SVF, stromal vascular fraction; LR, lactated ringer's.

<http://dx.doi.org/10.1016/j.burns.2015.05.004>

0305-4179/© 2015 Elsevier Ltd and ISBI. All rights reserved.

addition, ADRCs delivered with CBM showed increased blood vessel lumen area and blood vessel maturation at day 21 ($p = 0.05$). Interestingly, vascularity and overall cellularity within the CBM were 50% and 45% greater in animals receiving ADRC loaded scaffolds compared to CBM alone ($p < 0.05$).

Conclusions: These data demonstrate that seeding uncultured ADRCs onto CBM dermal substitute enhances wound angiogenesis, blood vessel maturation and matrix remodeling.

© 2015 Elsevier Ltd and ISBI. All rights reserved.

1. Introduction

Despite notable improvements in mortality rate, large burns continue to be associated with prolonged hospital stay and considerable morbidity [1]. For deep and extensive burns the use of conventional surgical techniques, such as autologous split thickness skin grafting is limited by donor site availability, frequently requiring the use of skin substitutes or temporary coverage with allogeneic or xenogeneic grafts. Numerous advances in tissue engineering have yielded a range of both natural and synthetic skin substitutes with applications for burns, diabetic wounds, ulcers and tissue reconstruction [2,3]. Importantly long-term viability of tissue-engineered skin substitutes requires the formation of neo-vessels allowing survival and integration after implantation [4].

Regenerative medicine using cellular therapy promises to improve our ability to treat and care for patients with burns. Indeed, stem cells have demonstrated potential as an adjunctive therapy to enhance wound healing [5–7]. In particular, the Stromal Vascular Fraction (SVF) of adipose tissue represents an innovative therapeutic strategy to promote tissue repair and regeneration [8]. The SVF is a heterogeneous cell population that contains endothelial cells, fibroblasts, smooth muscle cells, macrophages and adipose-derived stem cells [8,9]. Clinical-grade SVF has been referred to as Adipose Derived Regenerative Cells (ADRCs) [10]. A number of preclinical studies have shown that ADRCs have the capacity to promote angiogenesis and to modulate inflammation. Premaratne et al. [11] demonstrated increased vessel density and expression of pro-angiogenic growth factors along with reduced expression of pro-inflammatory factors in an animal model of chronic myocardial ischemia. Similarly, Feng et al. [12] showed reduced inflammatory response and improved survival in animals treated with SVF in an acute renal ischemia model. Others have evaluated the efficacy of ADRCs cells in hindlimb ischemia [13,14] as well as deep partial thickness burns [15]. Administration of ADRCs into/onto delivery scaffolds may provide a structural and biological matrix environment that increases cell survival and potentially accelerates the wound healing process. Therefore, development of novel delivery approaches to maximize their therapeutic effect is essential.

This study analyzed the delivery of ADRCs in conjunction with a collagen-based matrix (CBM) (i.e. Integra®). Integra® is a commercially available biosynthetic dermal regeneration template consisting of bovine collagen and chondroitin-6-sulphate,

with a silicone membrane backing which provides a barrier function. This CBM has been widely used in the clinical treatment of deep partial-thickness and full-thickness burn wounds [3,16]. Main reported disadvantages of Integra® include incidence of infection, cost, and delayed vascularization [17]. Therefore, improving vascularization, facilitating maturation of the newly-formed wound bed tissue, and shortening of the time needed before autograft application are from a clinical perspective highly desirable.

Given the pro-angiogenic and regenerative properties of ADRCs, we hypothesized that loading a CBM (i.e. Integra®) with ADRCs would overcome the delayed angiogenesis sometimes reported with this product and thereby accelerating the formation of a mature, well-vascularized wound bed suitable for the application of a skin graft. The purpose of this study was to test this hypothesis by evaluating whether seeding ADRCs onto CBM affects matrix properties and enhances wound healing after full thickness thermal burns.

2. Materials and methods

2.1. Porcine model of thermal burns

This study was conducted according to a research proposal approved by the Institutional Animal Care and Use Committee (IACUC). Eight (8) female Gottingen minipigs (5–6 months; 12–16 kg) were selected for this study. Swine were chosen as a preferred preclinical model of wound healing because of their anatomic and physiologic similarities to humans [18].

On day 0, each animal received ketamine/diazepam anesthesia with maintenance anesthetized state using isoflurane. The dorsum of each anesthetized animal was clipped and surgically scrubbed, prepped and draped. Six full thickness burns were induced on the dorsum of each animal; three on left side (designated L1, L2, and L3; cranial to caudal) and three on the right side (similarly designated R1, R2, and R3). Wounds were created by applying a pre-heated brass block (custom-made; 3.5 cm diameter; 350 g; heated to 180–200 °C) at a pressure of 0.4 kg/cm² on the dorsum of the animal for 1 min, using a custom built, calibrated device. The temperature of the block was verified using a laser thermometer immediately prior to each application. The burn procedure was validated to induce reproducible full thickness thermal burn (as assessed by histology) in the Gottingen strain of pig (data not shown). Burns (10 cm² each) were created 3.5 cm apart from each other and 4 cm away from the dorsal midline bilaterally. Reproducible positioning was facilitated by

use of a stencil template and markings prior to injury. Following induction of injury, burns were treated by topical application of a triple antibiotic cream (Water-Jel Technologies, Carlstadt, NJ) and covered with non-adherent bandage pads (Telfa bandage), held in place with Ioban (3M Corporation, St. Paul, MN) and elastic wraps. Pigs were allowed to fully recover from anesthesia and then returned to their pens.

Two days post injury animals were anesthetized and each wound site was excised under sterile technique to the level of the underlying muscular fascia. On the same day, each animal was randomized to receive either CBM seeded with freshly isolated autologous ADRCs ($n = 4$) or vehicle control CBM ($n = 4$) without ADRC's.

2.2. Adipose-derived regenerative cells (ADRCs) isolation

Two days after injury, prior to excision of burn wounds, animals were anesthetized with an intramuscular injection of 10 mg/kg ketamine with 2 mg/kg xylazine. Anesthetized state was maintained with inhalation of 3–5% isoflurane. Adipose tissue (16.8–26.6 g) was excised from the inguinal fat pad, minced, and then digested with Celase[®] enzyme (1 U/ml) (Cytos Therapeutics, San Diego, CA, USA) for 40 min at 37 °C. The ADRC fraction was separated by centrifugation at $600 \times g$ for 5 min and passed through 100- and 40- μ m Falcon[®] cell strainers (BD Biosciences, San Diego, CA, USA), sequentially. Cells were washed in Lactated Ringers Solution (LR) (3 times)

and were re-suspended at 5×10^6 cells/mL in LR. Total cell yield and cell viability were measured automatically with the cell counting device NucleoCounter[®] NC-100[™] (ChemoMetec).

2.3. ADRCs seeding onto collagen-based matrix for in vivo use

Within 30 min of isolation, ADRCs were directly loaded onto the CBM at a dose of 0.3×10^6 cm². For this purpose, 20×25 cm CBM sheets (Integra LifeScience Corporation, Plainsboro, NJ) were cut in 6 pieces of 5×5 cm (25 cm²) and placed in a 15 cm Petri dish with the silicone layer facing down. Next, 1 ml of ADRCs suspension was evenly loaded onto the CBM at a dose of $2.5 \times 10^5 \pm 25\%$ per cm² of CBM. Cells were then allowed to soak into and adhere to the matrix for 5–10 min prior to application onto the wound site. ADRC-loaded matrix was then placed onto the excised wound bed with the ADRC-loaded side in direct contact with the wound bed. The CBM for each wound was then was contoured and securely attached with staples onto the wound. The silicone layer was maintained throughout the entire course of the study (Fig. 1).

2.4. ADRCs characterization

Tissue samples from burned animals in the control group (not treated with ADRCs) were transported overnight to Cytos Therapeutics and processed, as described above.

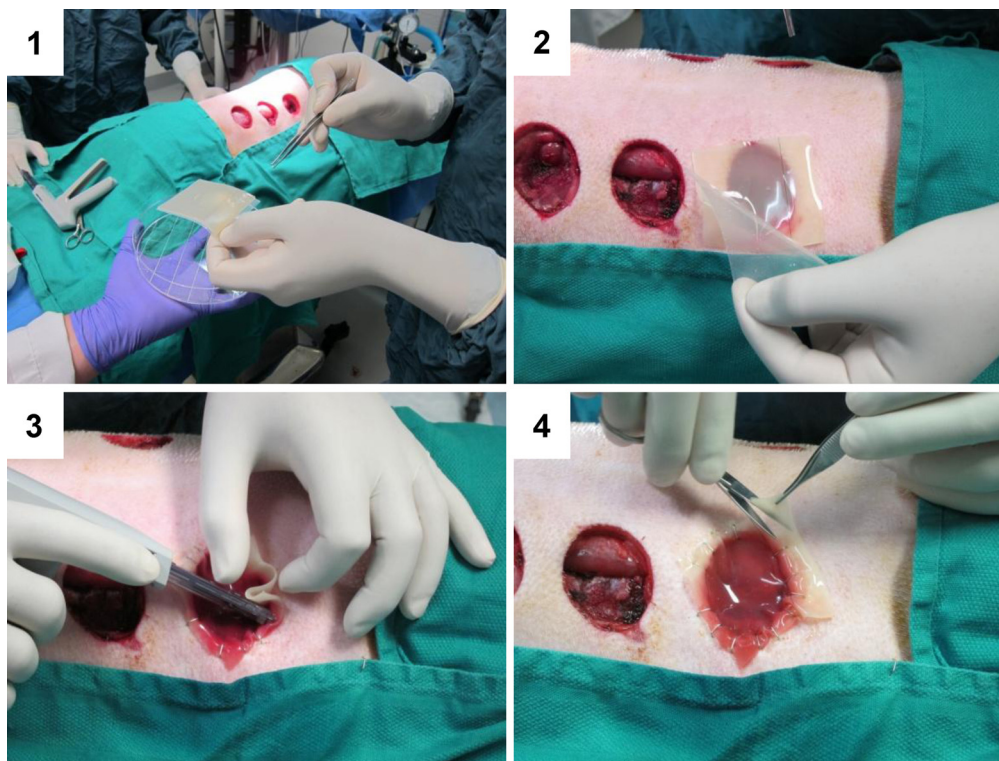


Fig. 1 – CBM application onto the excised burn wound site. CBM loaded with ADRCs was given to the surgeon (panel 1) and then placed onto the excised wound. The outermost layer of polyethylene was removed (panel 2). Then, the matrix was sized and shaped and secured to the wound site with surgical staples (panel 3). Additional shaping of CBM after stapling was performed as necessary (panel 4).

ADRCs were resuspended in staining buffer (0.2% BSA in PBS; BD Biosciences, San Diego) and then stained with the following antibodies CD45-FITC (clone K252.1E4; Serotec), CD31-PE (clone LCI-4; Serotec), CD90-PerCP-CyTM5.5 (clone 5E10; BD Biosciences) and CD146-PE (P1H12; BD Biosciences). After 20 min incubation at 4 °C, cells were washed twice in staining buffer and fixed using a BDFACS Lysis Solution (BD Biosciences). Acquisition and analysis of the cells were performed on FACSARIA using FACSDiva software.

2.5. Clonogenic assay

Freshly isolated porcine ADRCs were plated in 6-well plate at low density (100 cells/cm²) in DMEM/F12 containing 10% Fetal Bovine Serum (FBS). After 12–14 days, cells were rinsed with PBS, fixed with formalin, and stained with Hematoxylin solution (Hemacolor kit; EMD Millipore). Colonies containing >50 colony-forming unit fibroblasts (CFU-Fs) were counted. CFU-F frequency was calculated by dividing the number of colonies by the number of seeded cells.

2.6. In vitro assessment of ADRC biocompatibility with CBM

CBM pieces (8 mm diameter; 0.5 cm²) were placed in 48-well plate with the silicone layer facing down. Then, freshly isolated ADRCs resuspended in LR (0.25 × 10⁶/well/100 µl) were loaded onto the matrix. After 5 min of incubation, 500 µl of Endothelial Growth Medium (EGM2; Lonza) or DMEM/F12 containing 10% FBS was added into each well. The medium was replaced after 3 days of culture. Collagen-based matrices loaded with cells were harvested at day 1 and day 7. Scaffolds were fixed with 10% formalin and then embedded in OCT compound (Tissue-Tek) and frozen at –80 °C. Frozen specimens sections (15–20 µm) were prepared, fixed with ice-cold acetone and stained with hematoxylin & eosin (H&E). Scaffold sections were examined using light microscopy (Olympus BX-61).

Adherent ADRCs subsets were detected by immunostaining with anti-CD31 (Abbiotec), anti-CD45 (BD Biosciences), anti-CD90 (BD Biosciences) and anti-CD34 (Abcam). Briefly, CBM sections were blocked with CAS blocking buffer (Life Technologies) followed by incubation with primary antibodies CD31, CD45, CD90 or CD34. Sections were then incubated with a secondary antibody conjugated to an AlexaFluor[®] 555 (Life Technologies). Nuclei were stained with 4',6-diamidino-2-phenylindole (DAPI) (Life Technologies). Scaffold sections were examined using fluorescence microscopy (Zeiss Axioskop 40).

2.7. In vitro adhesion onto collagen-based matrix

CBM pieces (6 mm diameter; 0.3 cm²) were placed in 96-well black plate. Freshly isolated ADRCs were labeled with CM-Dil red dye (5 µg/ml; Life Technologies) and then resuspend in DMEM containing 1% FBS. Cells (0.25 × 10⁶/well/200 µl) were allowed to adhere to CBM or non-coated wells (negative control) for 20, 40 and 60 min at 37 °C. Wells were gently washed with PBS and fluorescence of adhering cells was measured using a microplate reader at excitation/emission

wavelengths of 544/590 nm (SpectraMax Gemini XS, Molecular Devices).

2.8. Planimetry wound imaging

For all animals, digital imaging of wounds was conducted on day 0 (post-burn), day 2 pre- and post-excision, day 7, day 14, day 21 and day 28 post thermal burns. All wounds were subjected to high quality digital imaging using the SilhouetteStar Wound Camera (ARANZ Medical, Christchurch, New Zealand). Wound images were then reviewed and total wound area was measured using the SilhouetteStarTM System.

2.9. Wound histology

Wound tissues from biopsies collected at day 7, 14 and 21 post-injury were fixed in 10% neutral-buffered formalin (NBF), embedded in paraffin, sectioned (5 µm), and stained with hematoxylin and eosin (H&E) and Masson Trichrome stain.

Entire slides were then digitally scanned using the Aperio ScanScope AT2 slide scanner (Aperio Technologies). Slides were viewed and analyzed remotely using the web-based ImageScope viewer. The Deconvolution Analysis algorithm package and ImageScope analysis software (version 12.1; Aperio Technologies) were applied to quantify histochemical staining. The software algorithm makes use of a deconvolution method to separate different colors, so that quantification of individual stain is possible without cross contamination. This algorithm calculates the percentage of weak (1+), medium (2+), and strong (3+) collagen positive staining. Employing this technique, a collagen deposition score was calculated by a simple formula involving the positive percentages (Score = 1 × [%Weak] + 2 × [%Medium] + 3 × [%Strong]).

Wound tissue thickness was measured as the distance between the tissue beneath the matrix and the dermal-adipose layer junction. A total of three to five measurements were performed using the measure tool of the ImageScope Software (version 12.1, Aperio Technologies).

2.10. Histopathology analysis

Histopathology was independently assessed by an experienced pathologist blinded to both protocol and treatment. Wound Tissue Maturation was scored according to the following scale: 0 normal tissue organization; (1) minimal disorganization; (2) mild disorganization; (3) moderate disorganization; (4) marked disorganization; (5) severe disorganization.

2.11. Immunohistochemistry

Tissue specimens were fixed in 10% normal buffered formalin and subsequently embedded in paraffin. Paraffin-embedded tissue sections (5 µm) were deparaffinized and re-hydrated through alcohol to water. Next, sections were incubated with BLOXALL Solution (Vector Laboratories) for 10 min to inactivate endogenous alkaline phosphatase activity. Tissue sections were then subjected to an antigen retrieval step by boiling sodium citrate solution (pH 6, Vector Laboratories) for 15 min in a pressure cooker. Polyclonal rabbit CD31 (5 µg/ml,

Table 1 – Adipose tissue harvest and adrc isolation characteristic.

Treatment	ID	Adipose tissue harvested (g)	Cell yield ($\times 10^6$ /g of fat adipose tissue)	Cell yield ($\times 10^6$)	Viability (%)
CBM + ADRCs	255	26.6	2.3	61.5	92.6
CBM + ADRCs	256	16.8	1.6	26.8	84.7
CBM + ADRCs	257	20.2	1.3	26.6	87.0
CBM + ADRCs	258	15.7	3.2	50.6	93.0
Mean \pm SD		19.8 \pm 4.9	2.10 \pm 0.8	41.3 \pm 17.5	89.3 \pm 4.0
CBM: collagen-based matrix.					

Abbiotec) and α -Smooth Muscle Actin (α -SMA, 2 μ g/ml, Abcam) antibodies were used for immunodetection of blood vessels on paraffin-embedded skin sections. Alkaline Phosphatase (AP)-based detection of the primary antibody was performed using a Vectastain ABC-AP kit (Vector Laboratories) according to the manufacturer's instructions, followed nuclear staining with Harris hematoxylin. As controls, tissue sections were stained as previously described without adding primary antibody.

CD31 and α -SMA stains were quantified using ImageScope analysis software (Microvessel Analysis Algorithm; Aperio). In each biopsy, annotations were created on the slides to demarcate the superficial and mid/deep regions of granulation tissue. The number of vessels per surface area, and the mean vessel lumen area were calculated using the micro-vessel analysis algorithm (Aperio Technologies).

2.12. Statistical analysis

Results are expressed as means \pm SEM or means \pm SD for graphs and tables, respectively. Comparisons between two groups were performed using an unpaired t-test (Graph Pad Prism version 6.03). A value of $p < 0.05$ was considered significant.

3. Results

3.1. Gottingen minipig adipose-derived regenerative cells isolation, viability, characterization and seeding onto CBM

ADRCs were successfully isolated from the inguinal fat pads of female Gottingen minipigs. An average of $2.1 \times 10^6 \pm 0.83 \times 10^6$ ADRCs was obtained per gram of processed adipose tissue (range: 1.3×10^6 – 3.2×10^6 cells/g tissue). The mean recovered cell viability from ADRC preparations was $89.3\% \pm 4.1\%$; ranging from 84.7% to 93.0% (Table 1).

Flow cytometric evaluation of these cells showed that leukocytes (CD45⁺) comprised an average of $\sim 24.5\%$ of ADRCs (range from 6.4 to 46.6%). Endothelial cells (CD31⁺/CD45[−]) averaged 9.7% of ADRCs (range from 1.9 to 19.1%) and stromal cells (fibroblast and fibroblast-like; CD90⁺/CD45[−]) averaged around 24.45% (range from 9.6 to 54.2%). Smooth muscle-related cells (SMCs; CD31[−]/CD146⁺/CD45[−]) accounted for around 26% of ADRCs (range 11.9 to 41.1%) (Table 2). In addition, using the colony-forming unit fibroblasts assay (CFU-F), we observed that the frequency of stromal progenitor/stem cells ranged from 0.2 to 5.6%.

To determine the interaction of ADRCs interaction within the pores of the CBM, ADRCs were seeded onto the matrix and optical microscopy analysis was performed at 1 and 7 days post-seeding. In vitro examination revealed that ADRCs are able to adhere, attach and spread onto the CBM (Supplementary Fig. 1). In addition, we observed that CBM supports greater ADRCs adhesion than control condition (non-coated wells) (Fig. 2A). This observation led us to evaluate which ADRCs subsets can adhere to the CBM. Immunofluorescence analysis showed that CD34, CD31, CD45 and CD90-positive cells adhered to CBM demonstrating that all major populations within ADRCs have the ability to interact to CBM (Fig. 2B).

3.2. Animal health and gross wound observations

All animals survived the study period. All treatments were well tolerated by the animals, and no evident side effects were observed in the control and treatment group. No differences in either body weight or body temperature was noted between control and treatment groups.

Representative images showing wound healing progression in ADRCs-loaded CBM and vehicle-loaded CBM are shown Fig. 3. There was no significant difference in mean contraction rate determined by planimetry analysis between the ADRC-loaded matrix and vehicle-loaded matrix (Supplementary Fig. 2). At day 7, wound contraction was minimal ranging from 2% to 3% in average. Wound contraction increased by about 25%, 40% and 53% at day 14, 21 and 28, respectively (Supplementary Fig. 2).

3.3. Wound histology observations

Histologic assessment of biopsies taken from wounds at early time points revealed successful integration of the CBM to the

Table 2 – Porcine ADRCs characterization.

Cell Population	Percent of positive cells within ADRCs (Mean \pm SD)
Leukocytes CD45 ⁺	24.5 \pm 14.2
Endothelial cells CD31 ⁺ /CD45 [−]	9.7 \pm 5.25
Stromal cells CD90 ⁺ /CD45 [−]	24.4 \pm 14.2
Smooth muscle-like cells CD146 ⁺ /CD45 [−] /CD31 [−]	26 \pm 11

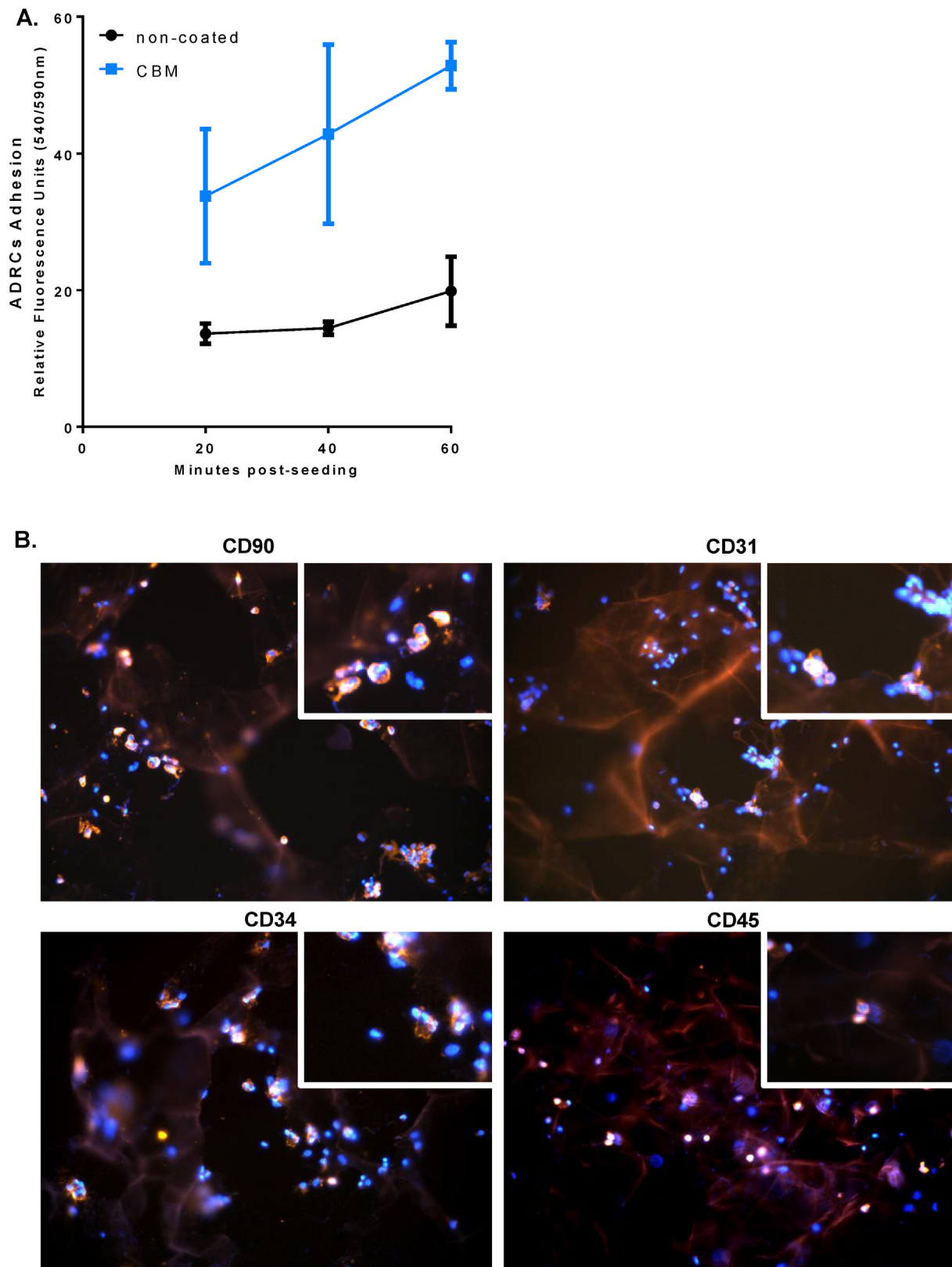


Fig. 2 – ADRCs adhesion onto CBM. (A) CM-Dil-labeled ADRCs were subjected to adhesion onto CBM-coated wells and non-coated wells. The fluorescence of adherent cells was quantified. (B) Freshly isolated ADRCs were allowed to adhere overnight onto CBM then stained with CD90, CD31, CD34 and CD45 antibodies (red fluorescence). Nuclei were stained with DAPI (blue fluorescence). Insets: magnification showing positive staining. Results are presented as mean \pm standard error of mean (SEM).

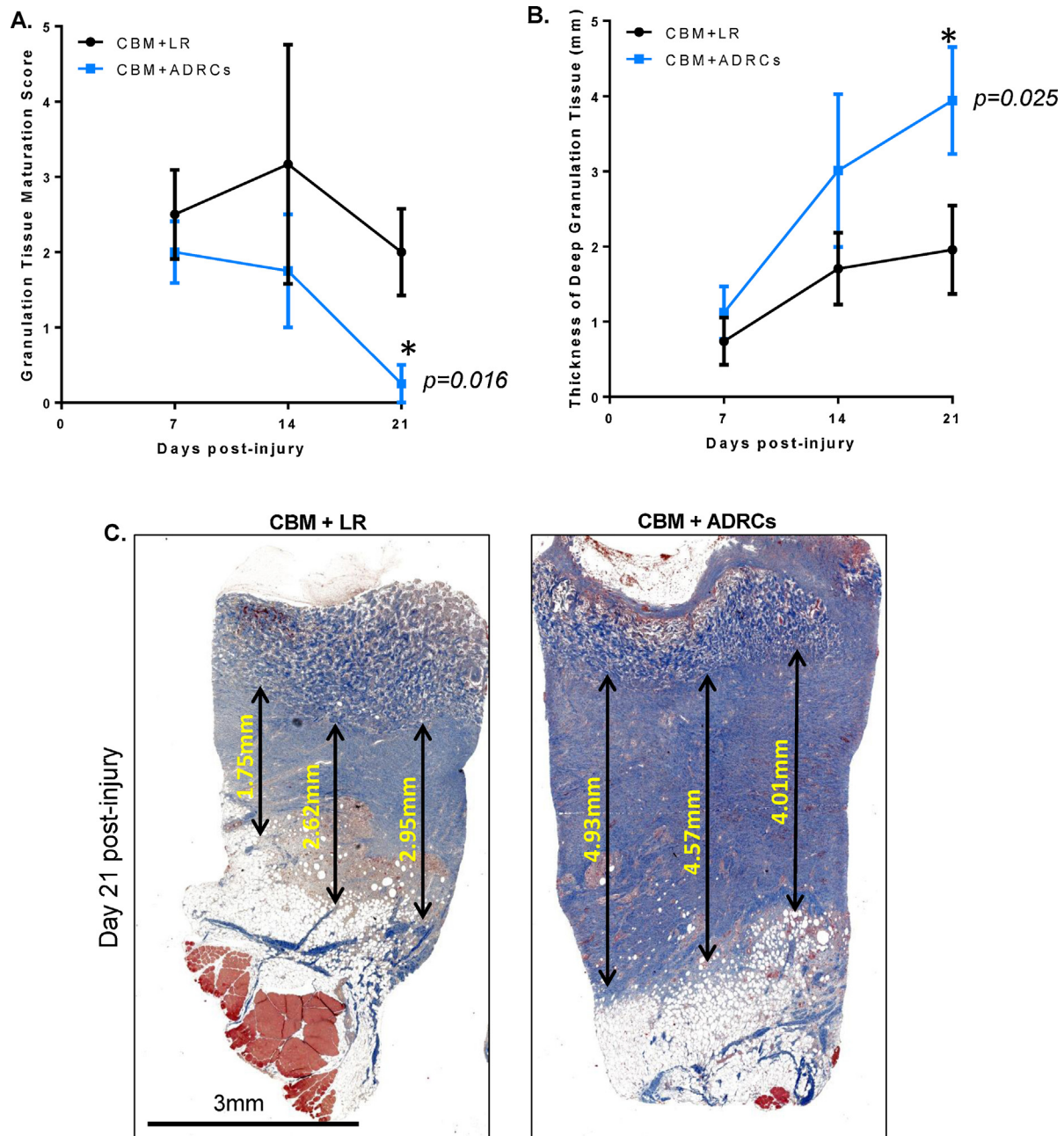


Fig. 3 – Histopathological analysis of the granulation tissue maturation beneath the CBM. (A) Biopsy histology was scored by an independent pathologist blinded to wound treatment using the following scale: 0 = normal organization; 1 = minimal disorganization; 2 = mild disorganization; 3 = moderate disorganization; 4 = marked disorganization and 5 = severe disorganization. (B) The graph represent the mean granulation tissue thickness in animals receiving CBM seeded with ADRCs (blue bar) or its control vehicle (black bar). (C) Representative photomicrographs of Masson Trichrome staining showing dermal tissue with three measurement markings. * $p < 0.05$; $n = 4$ animals/group. Results are presented as mean \pm standard error of mean (SEM).

wound bed. In this respect, the wound bed can be separated into two regions: the area within the CBM and the area below the CBM (referred to herein as wound bed tissue), up to the dermal-adipose junction.

Histologic scoring by an experienced study blinded pathologist assessing tissue organization revealed accelerated maturation of wound bed tissue in those wounds treated with

ADRCs-loaded CBM as compared to those treated with vehicle-loaded CBM (Fig. 3A). Accelerated tissue maturation was associated with the presence of a nearly normal dermis with mature collagen and blood vessels accumulation.

This finding led us to investigate the thickness of the wound bed beneath the CBM. The average depth of the wound bed tissue on day 21 post injury (day 19 after treatment) was

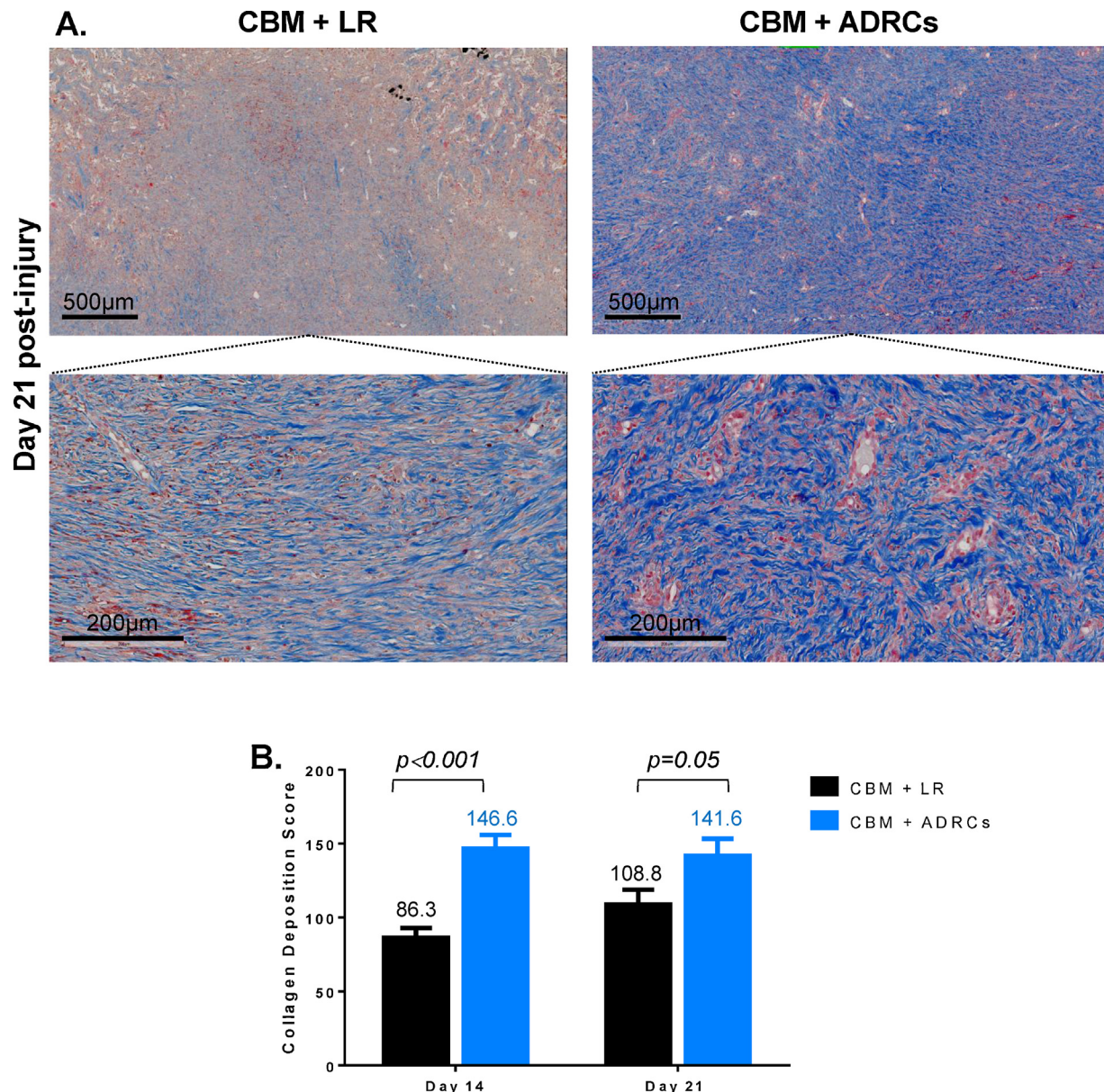


Fig. 4 – Digital quantification of collagen deposition within the wound bed. (A) Skin biopsies collected from animals receiving CBM + LR or CBM + ADRCs were stained for Masson Trichrome (MTC). Representative photomicrographs of sections stained with MTC at day 21 are shown. Images were collected from the mid/deep region granulation tissue of each wound. **(B)** Collagen deposition was quantified using automated positive pixel analysis of digitally scanned slides. $n = 4$ animals/group; 6 wounds for each treatment condition. Results are presented as mean \pm standard error of mean (SEM).

significantly greater (102% increase) in animals treated with ADRCs-loaded matrix compared to vehicle-loaded matrix (3.94 ± 0.71 mm vs. 1.95 ± 0.58 mm; $p = 0.025$) (Fig. 3B and C).

In order to confirm histopathological analysis, the degree of collagen deposition within the wound bed was assessed using Masson's trichrome (MTC) staining, as increased, organized collagen deposition is associated with improved wound bed maturation. Examples of wound tissue stained with MTC can be observed in Figs. 3C and 4A. Digital quantification of positive collagen pixels indicated that collagen deposition score was significantly increased (1.7-fold) in wounds treated with ADRCs-seeded CBM compared to those treated with

vehicle-seeded CBM at day 14 (146.9 ± 9.3 vs. 86.3 ± 6.6 ; $p < 0.001$) and day 21 (108.8 ± 10.1 vs. 141.6 ± 11.7 ; $p = 0.05$) (Fig. 4B).

Neovascularization is another key process promoting wound maturation and healing [19]. Therefore, blood vessel formation was quantified by establishing the number of CD31 positive vessels within the wound bed tissue on experiment days 14 and 21 post-injury using immunohistochemical digital analysis. Blood vessel density in the wound bed was 50% to 69.6% greater in wounds receiving ADRCs-loaded CBM compared to those treated with vehicle-seeded CBM at day 14 (212.1 ± 69.4 vs. 125.1 ± 54.4 vessels per mm^2 ; $p = 0.08$) and

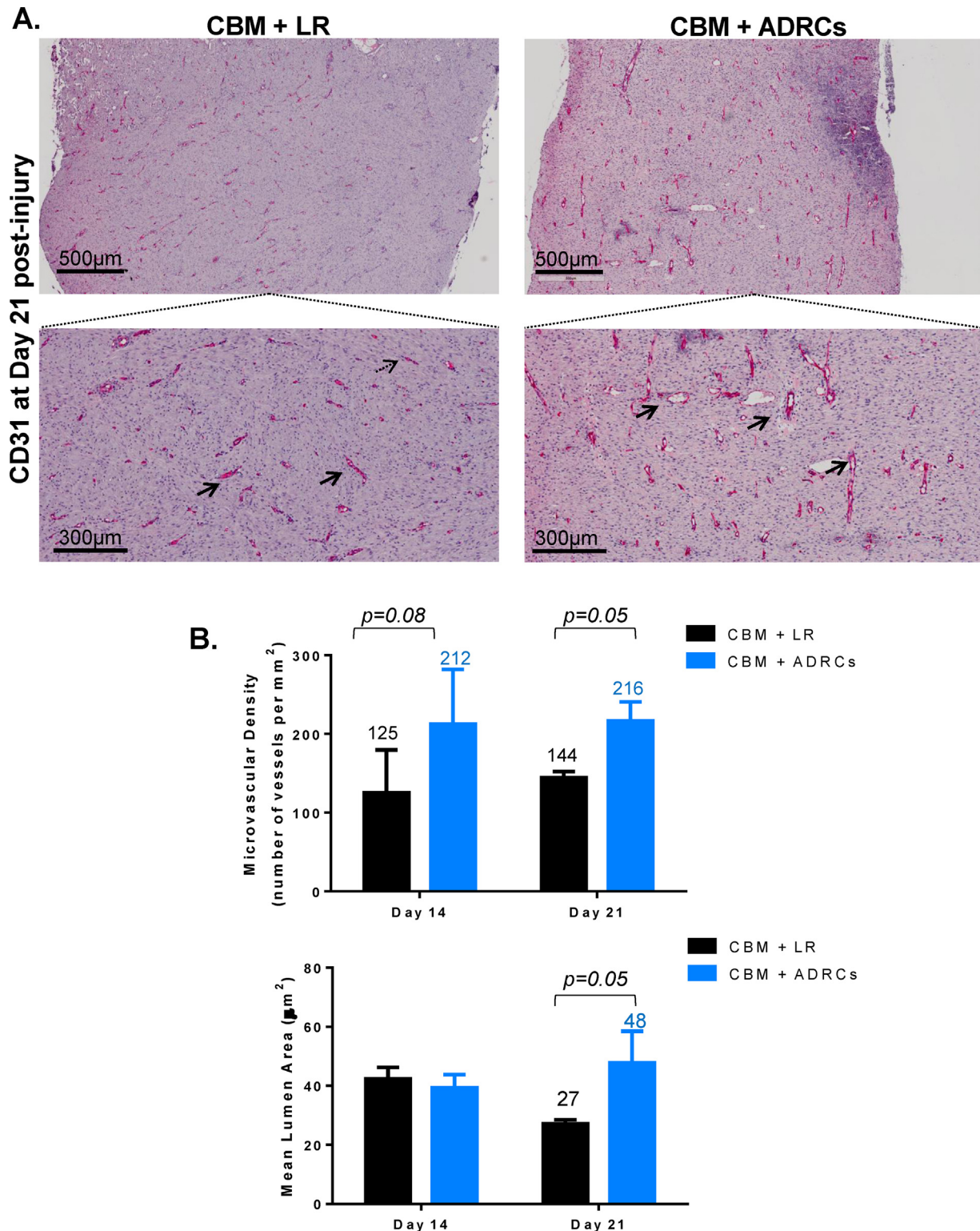


Fig. 5 – Quantitative analysis of new vessel formation in wound tissue. (A) Skin biopsies collected from animals receiving CBM + LR or CBM + ADRCs were stained for CD31. Representative photomicrographs of sections stained with CD31 are shown. Images were collected from the mid/deep region granulation tissue of each wound. **(B)** Microvessel density (MVD) and Lumen area were quantified using automated analysis of digitally scanned slides. $n = 4$ animals/group; 6 wounds for each treatment condition. Results are presented as mean \pm standard error of mean (SEM).

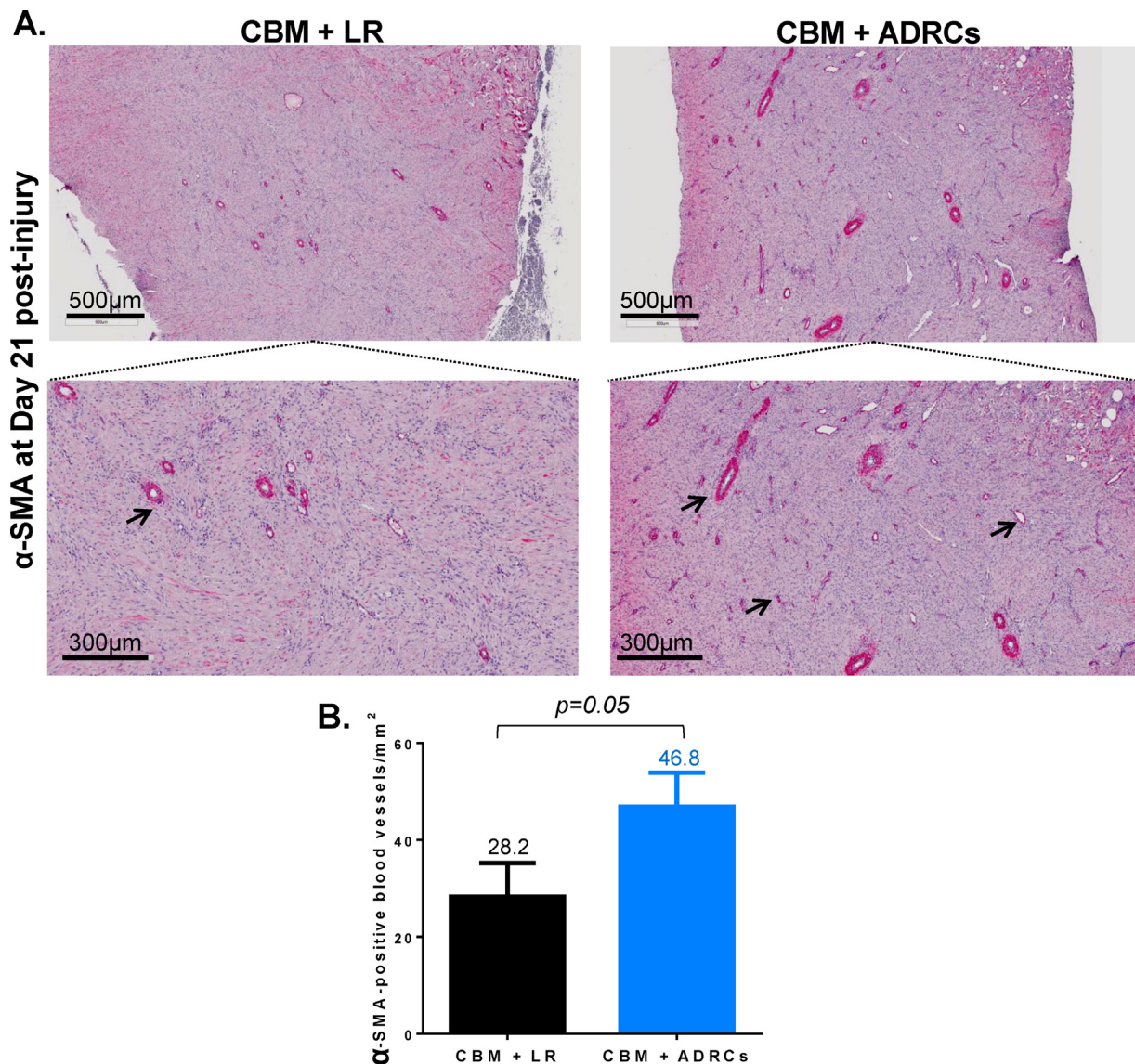


Fig. 6 – Quantitative analysis of α -SMA positive blood vessel in wound tissue on day 21. (A) Skin biopsies collected from animals receiving CBM + LR or CBM + ADRCs were stained for α -SMA. Representative photomicrographs of sections stained with α -SMA are shown. Images were collected from the mid/deep region granulation tissue of each wound. **(B)** The number of α -SMA-positive vessels was quantified using automated analysis of digitally scanned slides. $n = 4$ animals/group; 6 wounds for each treatment condition. Results are presented as mean \pm standard error of mean (SEM).

day 21 (216.3 ± 24.3 vs. 144.4 ± 7.6 vessels per mm^2 ; $p = 0.05$) (Fig. 5). Interestingly, the mean vessel lumen area at day 21 in the mid and deep dermis was 76.2% larger in wounds treated with ADRCs-loaded CBM than wounds receiving vehicle-loaded CBM (47.85 ± 10.68 vs. $27.15 \pm 2.3 \mu\text{m}^2$; $p = 0.05$) (Fig. 5). These observations led us to investigate the presence of mature blood vessels within the wound tissue. Immunohistological analysis of wound tissue sections stained with an anti- α SMA antibody revealed an increase in the number of α SMA-positive blood vessels in animals treated with ADRCs-seeded CBM compared to control treatment (46.8 ± 7.01 vs. 28.2 ± 7 vessels per mm^2 ; $p = 0.05$) (Fig. 6). These results demonstrated that seeding uncultured ADRCs onto CBM enhanced angiogenesis and blood vessel maturation.

We next sought to evaluate whether ADRCs modulate CBM matrix vascularity. Digital analysis of CD31 positive cells within the CBM itself showed that blood vessel density within CBM was 82% and 50% greater in ADRC-loaded scaffolds compared to CBM alone at day 14 (86.5 ± 8.5 vs 47.5 ± 13 vessels per mm^2 ; $p = 0.012$) and day 21 (86.4 ± 14.3 vs 57.3 ± 10.6 vessels per mm^2 ; $p = 0.06$), respectively (Fig. 7A and B). Interestingly, the improved vascularity observed in ADRCs-seeded CBM was associated with an increase in overall cellularity within the CBM. As shown in Fig. 7B and C, digital analysis showed that the number of nuclei per surface area was increased within the matrix supplemented with ADRCs compared to control LR vehicle at day 21 (1786 ± 244.3 vs. 1228 ± 195.6 nuclei per mm^2 ; $p = 0.044$) (Fig. 7A and C). This

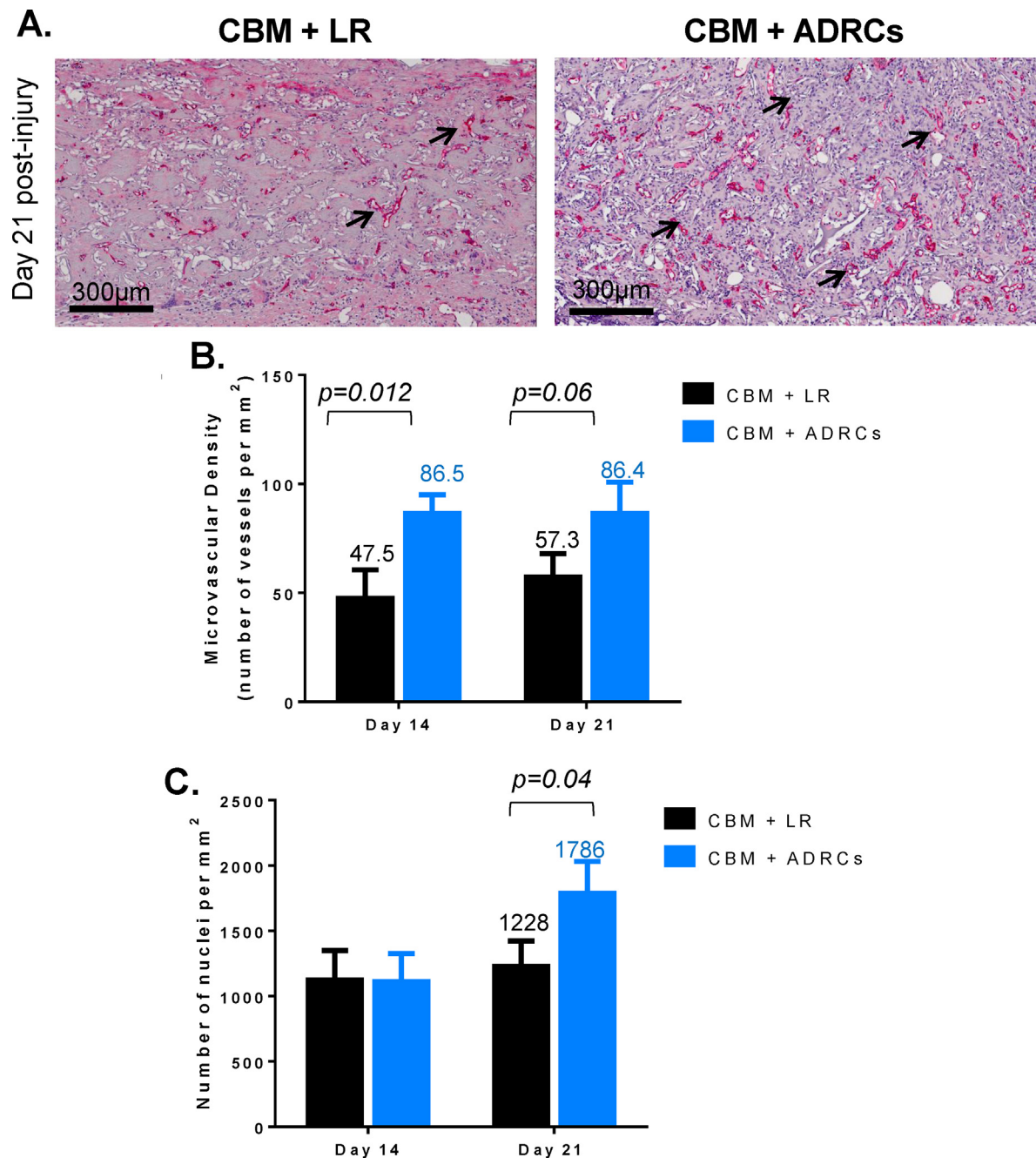


Fig. 7 – CBM vascularity and cellularity on day 21. (A) Skin biopsies collected from animals receiving CBM + LR or CBM + ADRCs were stained for CD31. Representative photomicrographs of sections stained with CD31 within CBM are shown. (B) Microvessel density (MVD) and number of nuclei were quantified using automated analysis of digitally scanned slides. $n = 4$ animals/group; 6 wounds for each treatment condition. Results are presented as mean \pm standard error of mean (SEM).

observation was confirmed by measuring the percent of matrix filled by cellular components using the deconvolution algorithm on Masson Trichrome staining. Digital analysis revealed that ADRCs loaded onto CBM statistically enhanced matrix filling compared control vehicle at day 21 post-injury ($74.5\% \pm 5.9$ vs. 50.1 ± 5.8 nuclei per mm^2 ; $p = 0.026$) (Supplementary Fig. 3).

Taken together, these data demonstrate that seeding ADRCs onto an off-the-shelf dermal substitute is a novel

viable clinical option to improve wound angiogenesis, blood vessel maturation and collagen deposition.

4. Discussion

Although improvements in burn management and care have significantly reduced overall mortality, there remains a critical need for novel avenues of improving the overall healing

process in order to optimize functional and aesthetic outcomes. Cell therapy has emerged as a promising new approach to promote wound healing, replace damaged skin and promote skin regeneration [5–9]. Adipose tissue and ADRCs/SVF cells are of particular interest due to the accessibility of tissue through a minimally invasive liposuction procedure or derived from the eschar itself because of the high frequency of cells with regenerative capacity within the population [20,21]. ADRC therapy has been evaluated in several clinical trials as a means to promote tissue repair [8,22–24]. The current study represents an effort to expand upon these potentially beneficial attributes into the treatment of full thickness contact burn wounds, *e.g.*, where grafting is required.

The utility of Integra as a scaffold for delivery of certain cell populations in the treatment of burn wounds has been investigated [25–28]. It is generally accepted that histogenesis begins at the base of the CBM where new blood vessels form. Layer by layer, from base to silicone, a progressive vascularization allows the process to occur at higher levels of the matrix [29]. Neovascularization and formation of well-organized, mature tissue beneath and within CBM is a key factor in the clinical use of this product. Specifically, the change in color observed as this process progresses (from white native to a peach or coral color as vascularized tissue develops) is used as the primary indicator of when it is appropriate to remove the silicone backing and apply the skin graft. Interestingly, it has been shown that full vascularization of the neodermis appeared at 4 weeks after CBM application [17]. The data herein demonstrate that seeding ADRCs onto CBM improves angiogenesis and final wound maturation. The effects of seeding ADRCs on CBM may improve current burn therapy, as more rapid vascularization has the potential to permit earlier application of the STSG, and/or mediate more robust retention of the STSG due to an improved quality of the tissue wound bed to which the graft is applied [30]. Consequently, loading ADRCs onto CBM may improve overall skin graft take, health, and perhaps overall clinical outcome.

ADRCs offer a novel approach to accelerate wound healing through their ability to integrate in the injured tissue and/or to release bioactive agents (such as VEGF, SDF-1, HGF, etc.) favoring tissue repair and regeneration [8–15,31,32]. In this study, we found that seeding uncultured ADRCs onto CBM increased local vascularization of the wound bed tissue, both beneath and within the CBM itself. Importantly, to our knowledge, we demonstrated for the first time that uncultured ADRCs may also promote maturation of blood vessels in a biosynthetic construct.

In this respect, key dynamic interactions occur between endothelial cells and mural cells (for example, pericytes) to affect vessel remodeling, diameter, as well as vascular basement membrane matrix assembly, a fundamental process necessary for vessel maturation and stabilization. These processes are critical to control the development of the functional microcirculation [33]. Of particular note, our findings also strongly suggest that ADRCs may modulate the CBM itself by increasing matrix maturation and cellularity. These data suggest that ADRCs loaded onto CBM may orchestrate the complex process of neovascularization by not only promoting angiogenesis but also blood vessel maturation. Nevertheless, further investigations are needed to decipher the role of ADRCs during vessel maturation.

Seeding ADRCs onto CBM appears to be both safe and feasible with no significant adverse systemic health effects over the course of the in life study period and no deleterious effects of ADRCs on the ability of CBM to resist wound contraction.

Our data suggest that seeding uncultured ADRCs onto this dermal substitute enhances tissue integration by increasing blood vessel formation, maturation and matrix remodeling. These results provide new insights for novel strategies for skin regeneration after thermal burns, consisting of the combination of ADRCs with engineered biomaterials. Utilizing uncultured population of cells may facilitate potential clinical application. Further development of matrix scaffold engineered with ADRCs may lead to improved healing in future clinical trials.

Conflict of interest statement

PF, SB, AG, ZA, SZ and JKF are paid employees and stock holders of Cytori Therapeutics, Inc., San Diego, CA. MT is receiving consulting fees from Cytori Therapeutics, Inc. CB and IH have no conflicts of interest with regard to this study.

Acknowledgements

This work was supported by contract HHSO100201200008C from the Biomedical Advanced Research and Development Authority (BARDA), Department of Health and Human Services.

The authors would also like to thank Dr. Kathy Mekjian and Dr. Steven Kesten for their valuable comments and suggestions to improve the manuscript.

Appendix A. Supplementary data

Supplementary data associated with this article can be found, in the online version, at <http://dx.doi.org/10.1016/j.burns.2015.05.004>.

REFERENCES

- [1] National Burn Repository. NBRannualreport.pdf. American Burn Association; 2014. (<http://www.ameriburn.org/2014>).
- [2] Shahrokhi S, Arno A, Jeschke MG. The use of dermal substitutes in burn surgery: acute phase. *Wound Repair Regen* 2014;22(1):14–22.
- [3] Veen VC, van der Veen VC, Wal MBA, Leeuwen MCE, Ulrich MMW, Middelkoop E, et al. Biological background of dermal substitutes. *Burns* 2010;36(3):305–21.
- [4] Kaully T, Kaufman-Francis K, Lesman A, Levenberg S. Vascularization-the conduit to viable engineered tissues. *Tissue Eng* 2009;15(2):159–69.
- [5] Jeschke MG, Finnerty CC, Shahrokhi S, Branski LK, Dibildox M. Wound coverage technologies in burn care: novel techniques. *J Burn Care Res* 2013;34(6):612–20.

- [6] Arno A, Alex Smith RH, Blit PH, Shehab al M, Gauglitz GG, et al. Stem cell therapy: a new treatment for burns. *Pharmaceuticals* 2011;4(10):1355–80.
- [7] Burd A, Ahmed K, Lam S, Ayyappan T, Huang L. Stem cell strategies in burns care. *Burns* 2007;33(3):282–91.
- [8] Kokai LE, Marra K, Rubin JP. Adipose stem cells: biology and clinical applications for tissue repair and regeneration. *Transl Res* 2014;163(4):399–408.
- [9] Zuk PA, Zhu M, Ashjian P, de Ugarte DA, Huang JJ, Mizuno H, et al. Human adipose tissue is a source of multipotent stem cells. *Mol Biol Cell* 2002;13(12):4279–95.
- [10] Fraser JK, Hicok KC, Shanahan R, Zhu M, Miller S, Arm DM. The celution[®] system: automated processing of adipose-derived regenerative cells in a functionally closed system. *Ad Wound Care* 2014;3(1):38–45.
- [11] Premaratne GU, Ma L, Fujita M, Lin X, Bollano E, Fu M. Stromal vascular fraction transplantation as an alternative therapy for ischemic heart failure: anti-inflammatory role. *J Cardiothorac Surg* 2011;6:43.
- [12] Feng Z, Ting J, Alfonso Z, Strem BM, Fraser JK, et al. Fresh and cryopreserved, uncultured adipose tissue-derived stem and regenerative cells ameliorate ischemia-reperfusion-induced acute kidney injury. *Nephrol Dial Transplant* 2010;25(12):3874–84.
- [13] Hao C, Shintani S, Shimizu Y, Kondo K, Ishii M, Wu H, et al. Therapeutic angiogenesis by autologous adipose-derived regenerative cells: comparison with bone marrow mononuclear cells. *Am J Physiol Heart Circ Physiol* 2014;307(6):H869–79.
- [14] Kondo K, Shintani S, Shibata R, Murakami H, Murakami R, Imaizumi M, et al. Implantation of adipose-derived regenerative cells enhances ischemia-induced angiogenesis. *Arterioscler Thromb Vasc Biol* 2008;29(1):61–6.
- [15] Atalay S, Coruh A, Deniz K. Stromal vascular fraction improves deep partial thickness burn wound healing. *Burns* 2014;40(7):1375–83.
- [16] Blackwood KA, McKean R, Canton I, Freeman CO, Franklin KL, Cole D, et al. Development of biodegradable electrospun scaffolds for dermal replacement. *Biomaterials* 2008;29(21):3091–104.
- [17] Moiemens NS, Vlachou E, Staiano JJ, Thawry Y, Frame JD. Reconstructive surgery with Integra dermal regeneration template: histologic study, clinical evaluation, and current practice. *Plast Reconstr Surg* 2006;117(7S):160S–74S.
- [18] Sullivan TP, Eaglstein WH, Davis SC, Mertz P. The pig as a model for human wound healing. *Wound Repair Regen* 2001;9(2):66–76.
- [19] Gurtner GC, Werner S, Barrandon Y, Longaker MT. Wound repair and regeneration. *Nature* 2008;453(7193):314–21.
- [20] Natesan S, Wrice NL, Baer DG, Debrided Christy RJ. Skin as a source of autologous stem cells for wound repair. *Stem Cells* 2011;29(8):1219–30.
- [21] Fraser JK, Wulur I, Alfonso Z, Hedrick MH. Fat tissue: an underappreciated source of stem cells for biotechnology. *Trends Biotechnol* 2006;24(4):150–4.
- [22] Casteilla L, Planat-Benard V, Laharrague P, Cousin B. Adipose-derived stromal cells: their identity and uses in clinical trials, an update. *World J Stem Cells* 2011;3(4):25–33.
- [23] Perin EC, Sanz-Ruiz R, Sánchez PL, Lasso J, Pérez-Cano R, Alonso-Farto JC, et al. Adipose-derived regenerative cells in patients with ischemic cardiomyopathy: the PRECISE Trial. *Am Heart J* 2014;168(1): 88–95.e2.
- [24] Houtgraaf JH, Wijn Dekker den WK, Dekker den K, van Dalen BM, Springeling T, et al. First experience in humans using adipose tissue-derived regenerative cells in the treatment of patients with ST-segment elevation myocardial infarction. *J Am Coll Cardiol* 2012;59(5):539–40.
- [25] Wood FM, Stoner ML, Fowler BV, Fear MW. The use of a non-cultured autologous cell suspension and Integra dermal regeneration template to repair full-thickness skin wounds in a porcine model: a one-step process. *Burns* 2007;33(6):693–700.
- [26] Meruane MA, Rojas M, Marcelain K. The use of adipose tissue-derived stem cells within a dermal substitute improves skin regeneration by increasing neoangiogenesis and collagen synthesis. *Plast Reconstr Surg* 2012;130(1):53–63.
- [27] Branski LK, Gauglitz GG, Herndon DN, Jeschke MG. A review of gene and stem cell therapy in cutaneous wound healing. *Burns* 2009;35(2):171–80.
- [28] Bhavsar D, Tenenhaus M. The use of acellular dermal matrix for coverage of exposed joint and extensor mechanism in thermally injured patients with few options. *Eplasty* 2008;8:e33.
- [29] Canonico S, Ferdin Campitiello O, Corte della AD, Padovano V, Pellino G. Treatment of leg chronic wounds with dermal substitutes and thin skin grafts. In: Gore M, editor. *Skin graft*. InTech; 2013. p. 1–26 (Chapter 5).
- [30] Greenwood J, Amjadi M, Dearman B, Mackie I. Real-time demonstration of split skin graft inosculation and integra dermal matrix neovascularization using confocal laser scanning microscopy. *Eplasty* 2009;9:e33.
- [31] Kapur SK, Katz AJ. Review of the adipose derived stem cell secretome. *Biochimie* 2013;95(12):2222–8.
- [32] Ebrahimian TG, Pouzoulet F, Squiban C, Buard V, Andre M, Cousin B, et al. Cell therapy based on adipose tissue-derived stromal cells promotes physiological and pathological wound healing. *Arterioscler Thromb Vasc Biol* 2009;29(4):503–10.
- [33] Lilly B. We have contact: endothelial cell-smooth muscle cell interactions. *Physiology* 2014;29(4):234–41.